18th IFHTSE CONGRESS
International Federation for Heat Treatment and Surface Engineering
IFHTSE
ANAIS
PROCEEDINGS
ISSN 1516-392X

# A COMPLETE MODEL FOR THE EFFECTS OF SILICON IN 5%Cr HOT WORK TOOL STEELS[1]

*Rafael Agnelli Mesquita*[2]
*Hans-Jürgen Kestenbach*[3]
*Celso Antonio Barbosa*[4]

**Abstract**
Recent modifications in chemical composition have been applied commercially to high alloy tool steels to improve toughness and tempering resistance. A common point in all compositions is the reduction of silicon content from the 1,0% used in AISI H11 and H13 down to 0.3% or lower levels. The present work investigates in detail the effect of silicon on tempering sequence and alloy carbide formation, proposing an explanation for the mechanical properties. Laboratory heats with silicon contents between 0.05 and 2.0% were cast and forged under industrial conditions. Mechanical tests were based on impact toughness and hardness measurements, after hardening from 1020ºC and tempering at temperatures between 400 and 650ºC. Secondary carbides were evaluated through transmission electron microscopy (TEM), mainly on extraction replicas, and matrix features were observed in thin foils. High resolution scanning electron microscopy was also applied, especially on fracture surface samples, to correlate toughness results with secondary carbide distributions. The effect of Si on cementite formation was found to be the major factor for the differences observed for the mechanical properties. During the initial tempering stages, cementite formation is delayed or inhibited in high Si steels, anticipating alloy carbide formation with preferred $M_7C_3$ precipitation on high energy interfaces. After longer tempering, $M_7C_3$ particles coarsen and may act as preferential cracking routes, explaining the lower toughness of high Si steels. In low Si steels, cementite is stabilized by Cr, Mo and V in solid solution, delaying alloy carbide precipitation and thus increasing tempering resistance.
**Key-words:** Silicon; Tool steels; Toughness; Secondary hardening; Precipitation; Phosphorous.

[1] *Technical contribution to the 18th IFHTSE Congress - International Federation for Heat Treatment and Surface Engineering, 2010 July 26-30th, Rio de Janeiro, RJ, Brazil.*
[2] *Professor, PhD, Universidade Nove de Julho, São Paulo, SP, Brazil, rafael.mesquita@uninove.br.*
[3] *Head of Research, Villares Metals, Sumaré, SP, Brazil, celso.barbosa@villares.com.br.*
[4] *Professor, PhD, Universidade Federal de São Carlos, SP, Brazil. dhjk@ufscar.br.*

## 1 INTRODUCTION

Hot work steels are applied in industry for several forming operations, especially in tools and dies for hot forging, extrusion or non-ferrous die casting. Due to properties and cost combinations, several compositions may be employed, being of special interest the 5%Cr hot work tool steels. This steel is widely used in hot working tools and dies, due to the proper combination of several properties, namely: hot strength, tempering resistance, toughness and thermal conductivity, without using extremely high amounts of alloy contents, which could impair cost-benefit evaluations.[1] Therefore, the 5%Cr hot work tool steels are considered to be the most important class of hot work steels that is currently applied in industry,[1] being well-known the AISI hot class grades H11 and H13.

H11 steel was the first grade used by industry, developed in the 1930's,[2,3] with (wt%) 0.4%C, 5%Cr, 1.2%Mo, 0.5%V, 1%Si. At that time, the addition of silicon to low alloy steels such as 4340 had been a quite new concept, used to promote higher tempering resistance and to reduce the effects of 350ºC tempered martensite embrittlement.[4] Classical papers[5-7] show that both effects are related to the slower formation of cementite when high silicon contents are present. Thus, it seemed only to be natural that the emerging new hot work steels should present high silicon contents, such as the 1 wt% Si of both the H11 and H13 (same composition as H11 but higher V addition) steels of that time.[1] On the other hand, more recent results from both scientific[8-11] and technological[12] investigations have shown that the reduction of silicon content from 1 wt% to 0.3 wt% or less leads to strong improvements in mechanical properties. This concept has mainly been applied to the H11 grade, and a new class of low Si modified H11 grades has emerged as the most important source for modern high quality hot work steels. Considering all these facts, the modification of silicon content in hot work steels may be considered to be one of the most relevant facts in the developments of new alloys for hot work tooling in the last 10 years.[13-18]

In spite of the importance of lower Si contents in recent tool steels, very few papers were dedicated to understand the reason for such modifications,[8-11] with only one paper addressing the role of carbide precipitation strengthening.[10] Due to their high temperature applications, the most important strengthening mechanism in hot work steels is the precipitation of alloy carbides at temperatures above 550ºC. It is therefore only natural to expect that the improvement in mechanical properties should be related to the effect of Si on precipitation hardening. Indeed, recent studies have shown that Si strongly affects the precipitation hardening aspects,[19] leading to different distributions of alloy carbides and modification of impact toughness.[20] It is the aim of the present paper to gather all the previous results and elaborate a reasonable model that may account for all the effects of Si in hot work steels. Due to the possible influence of phosphorous in these phenomena,[21] the synergy of phosphorous and silicon is also considered in the present model.

All the results presented were based on laboratory heats, produced industrially and using standard processing conditions for hot work steels. Four different levels of Si with two different phosphorous contents were analyzed. Mechanical properties and precipitation hardening were correlated by the use of transmission electron microscopy (TEM) and scanning electron microscopy (SEM), including high resolution observations of fracture surfaces.

## 2 EXPERIMENTAL PROCEDURE

Table 1 shows the chemical compositions of eight experimental steels which were prepared in a vacuum induction furnace as 50 kg ingots of 140 mm medium section width. After hot forging to a 70 mm square section size and homogenizing at 1260ºC for 20h, samples were subjected to a special commercial annealing cycle including austenizing, quenching, high temperature tempering and slow cooling, designed to obtain the most adequate microstructure for typical applications of these materials.[22]

**Table 1.** Chemical compositions of experimental steels in weight percent. The symbols "bP" indicate compositions with about 0.010%P, which is below the traditional content of 0.025%P

| | Steel | C | Si | Mn | Cr | Ni | Mo | W | V | Ti | Al | P | S ppm | N ppm | O ppm |
|---|---|---|---|---|---|---|---|---|---|---|---|---|---|---|---|
| ↑P | 1- 0,05Si | 0,35 | 0,05 | 0,36 | 5,02 | 0,20 | 1,27 | 0,09 | 0,42 | <0,005 | 0,028 | 0,026 | 35 | 18 | 32 |
| ↑P | 2- 0,30Si | 0,35 | 0,29 | 0,35 | 5,09 | 0,20 | 1,29 | 0,10 | 0,42 | <0,005 | 0,015 | 0,027 | 40 | 35 | 12 |
| ↑P | 3- 1Si | 0,36 | 0,98 | 0,35 | 5,03 | 0,19 | 1,30 | 0,10 | 0,41 | 0,006 | 0,023 | 0,026 | 35 | 39 | 21 |
| ↑P | 4- 2Si | 0,38 | 2,06 | 0,35 | 5,05 | 0,20 | 1,33 | 0,10 | 0,40 | 0,007 | 0,038 | 0,029 | 40 | 44 | 12 |
| ↓P | 5- 0,05 Si_bP | 0,36 | 0,06 | 0,35 | 4,99 | 0,22 | 1,31 | 0,11 | 0,42 | <0,005 | 0,022 | 0,011 | 40 | 33 | 15 |
| ↓P | 6- 0,3 Si_bP | 0,35 | 0,30 | 0,35 | 4,98 | 0,21 | 1,30 | 0,09 | 0,42 | <0,005 | 0,020 | 0,010 | 35 | 36 | 20 |
| ↓P | 7- 1Si_bP | 0,36 | 1,03 | 0,36 | 5,03 | 0,20 | 1,31 | 0,11 | 0,43 | 0,006 | 0,036 | 0,010 | 40 | 22 | 29 |
| ↓P | 8- 2Si_bP | 0,36 | 1,96 | 0,35 | 4,97 | 0,20 | 1,28 | 0,10 | 0,41 | 0,007 | 0,042 | 0,012 | 40 | 27 | 31 |

Commercial heat treatment conditions were simulated to prepare samples for mechanical testing and microstructural observations. After austenitizing at 1020ºC for 30 min, samples were oil quenched and double tempered at temperatures between 400 and 650ºC, followed by air cooling. For mechanical properties, transverse Charpy impact tests and hardness measurements were employed. Carbide distributions were investigated by TEM (Philips CM120 operated at 120kV), using carbon extraction replicas, complemented by EDS microanalysis of individual carbide particles. Extraction replicas were prepared following one of the procedures described in the literature.[10]

In order to study the initial formation of these carbides, some specimens were austenitized and quenched but samples were not fully tempered: they were removed from the tempering furnace just after the temperature had reached 625ºC for the first time. The average heating rate in this procedure was 20ºC/min. This condition is referred to in the text as 0 min at 625ºC tempering.

## 3 RESULTS

### 3.1 Mechanical Properties

Hardness and toughness results for all chemical compositions (see Table 1) are shown in Fig. 1, where several interesting effects of Si may be observed. First, after tempering at temperatures below 500ºC, Si has a very strong effect on hardness, increasing the hardness by about 8 HRC. Two causes are related to that, with almost the same importance in terms of hardness increase:[19] i) the classical effect of silicon in retarding cementite formation and thus retaining more carbon in solid solution in martensite; and ii) the contribution of Si to solid-solution hardening. In relation to toughness, the differences found may simply be attributed to the differences in hardness, as discussed in detail elsewhere.[20]

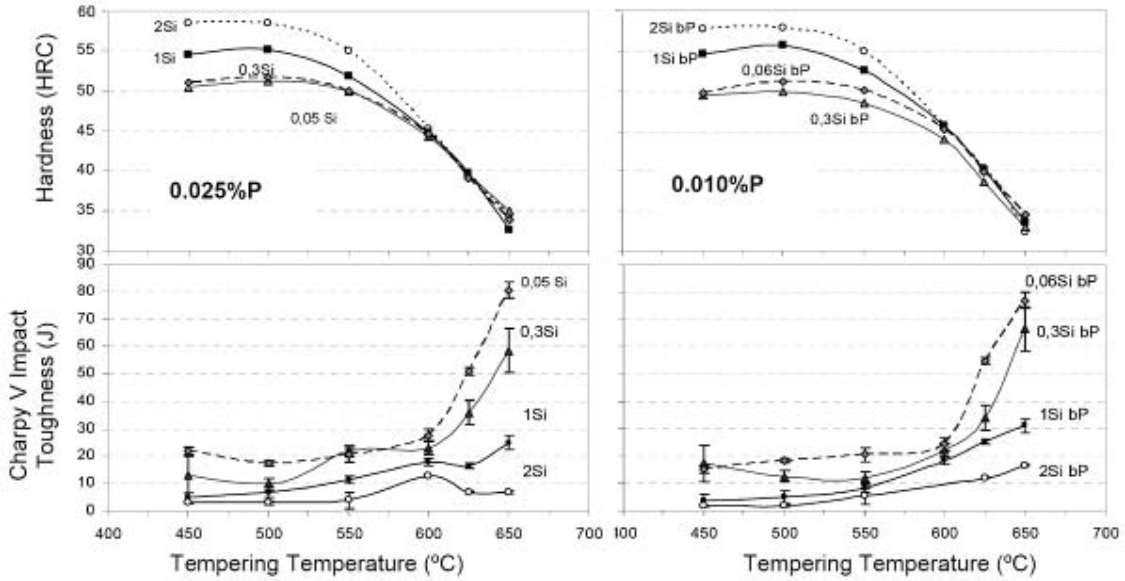


**Figure 1.** Comparison of tempered hardness and impact toughness for all compositions, with different Si contents and two P levels.

A second and very relevant observation concerns the mechanical properties after tempering at higher temperatures, above 600ºC. In such conditions, hardness values for all alloys are observed to be constant in terms of silicon content, but strong differences in toughness arise. For instance, at tempering temperatures of 625ºC (which are still in use for practical applications),[1] the differences in impact toughness from the usual 1%Si steel to the 0.3%Si steels (common content in new alloys) are more than 100%. And if the lowest and highest Si contents are considered (2.0% and 0.05%Si), such differences increase to more than 500%. Considering the importance of toughness in many tooling applications, such as die casting, these facts thus emphasize the strong benefits obtained from the new low Si steels.[23]

In relation to the P effect, another interesting fact may be observed (Fig. 2). The reduction of P content shows a strongly positive effect in high Si steels, but not in the low Si grades (considering that the high P levels are still below the maximum of 0.035%P accepted by the standard ASTM tool steel compositions). Thus, with respect to the high Si traditional grades, the reduction in P is in agreement with the literature,[24] showing the benefits of very low P levels in H11 and H13 steels. However, the same rule is shown to be much less important for the lower Si steels.

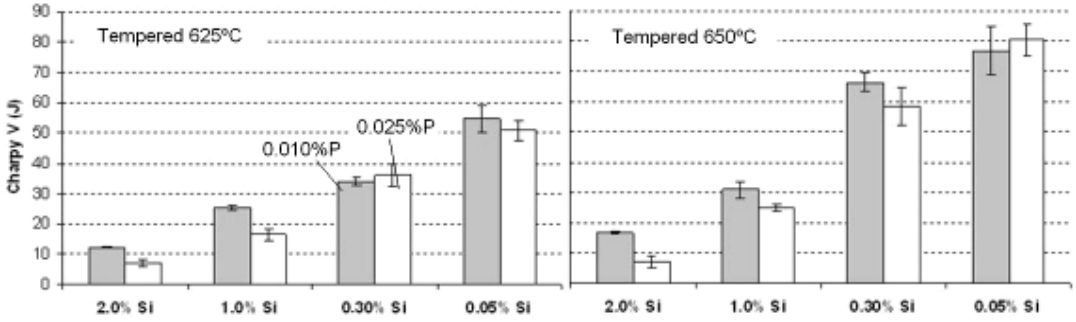


**Figure 2.** Comparison of low and high P H11 steels, for different Si levels and different tempering conditions.

As the toughness results after tempering above 600ºC are not possible to be explained by simple strength differences (i.e., the steels show in these conditions the same hardness) further detailed studies were carried out, as shown in the following sections.

### 3.2 Fractography

Fracture surfaces were observed for all steels, with results presented in Fig. 3 only for the lowest (0.05%) and highest (2.0%) Si contents; other results may be found in a previous paper.[19] All results observed are in agreement with the previous discussion of mechanical properties. After tempering below 600ºC, fracture surfaces of low and high Si steels have approximately the same appearance, of quasi-cleavage, transgranular with respect to austenite grains. However, after tempering at higher temperatures, low Si steels present an increase of dimpled ductile areas, in agreement with the reduction in hardness from 50HRC to 35 HRC according to Fig.1. For the high Si steels, on the other hand, fracture surfaces change from quasi-cleavage to principally intergranular type, delineating prior austenite grains, especially in the 0.025% P steel (left hand side, Figs. 3a and 3b). For the high Si low P grade, several intergranular areas are still observed, but cleavage and some ductile areas are also present (right hand side, Figs. 3a and 3b).

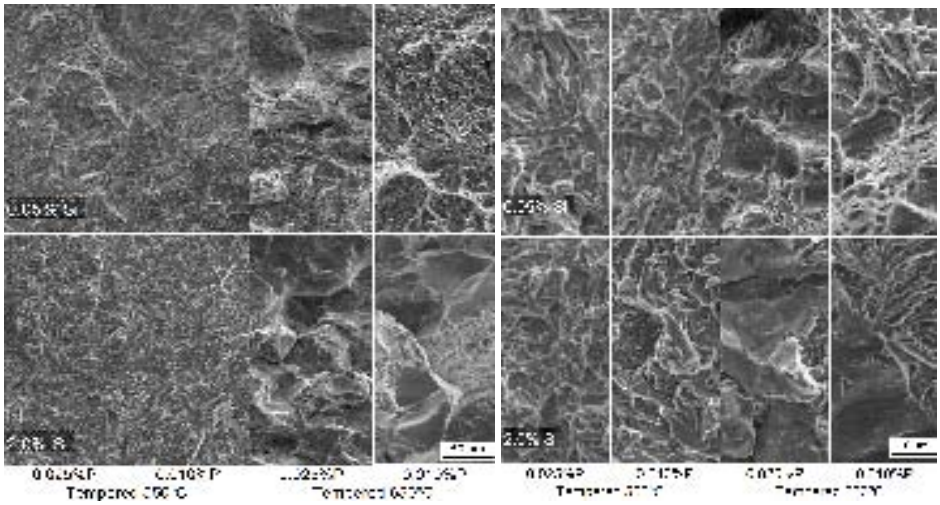

a) b)

**Figure 3.** a) Modification of fracture surfaces as a function of tempering temperature, for the higher and lower Si levels (200x magnification). b) details for low and high Si steels, under higher magnification (1000x).

To better understand these results, high resolution SEM observations are shown in Fig. 4. It can be seen that the intergranular areas of the high Si steels (with respect to austenite grain boundaries) are covered by particles (Fig. 4a). In other areas of the high Si steel, transgranular fractures (with respect to prior-austenite grains) are also present, but particles decorating fracture surfaces are still observed (Fig. 4b). The morphology and size of such regions allow to identify them as interfaces between martensite laths (shown in Fig. 5). It can therefore be concluded that, after tempering above 600ºC, fracture surfaces of the high Si steels are marked by the presence of particles of about 50-150 nm in size, leading to intergranular fracture either between prior-austenite grains or between martensite laths and packages. For low Si steels, most regions present ductile dimpled fractures, with no particles on the fracture surfaces (Fig. 4c).

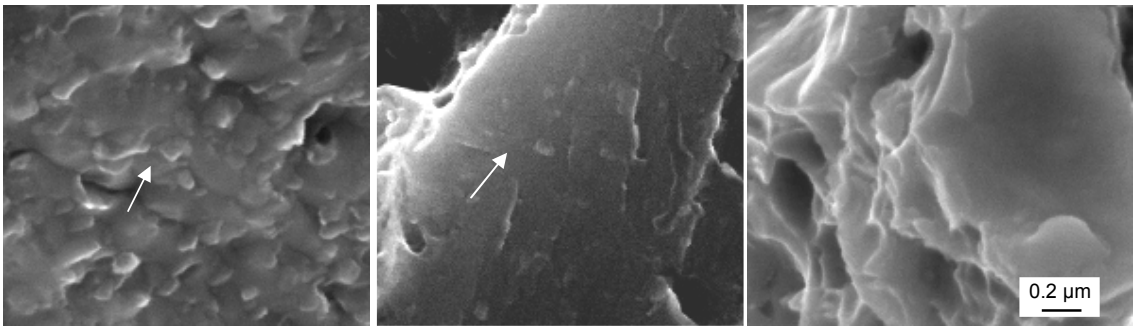


**a)** 2%Si **b)** 2% Si **c)** 0.05% Si

**Figure 4.** Examples of brittle and ductile fracture: a) Intergranular regions (with respect to austenite grains). b) Transgranular regions with respect to austenite grains, which are intergranular with respect to martensite laths; in (a) and (b), examples of carbide particles have been marked by arrows. c) Ductile regions of low Si steels, where no carbides are identified. All micrographs taken after hardening and tempering for 2x2h at 625ºC, yielding hardness levels of about 40 HRC.

### 3.3 Carbide Precipitation

The final correlation between properties and microstructure was based upon the different distributions and natures of the secondary hardening carbides, as shown in Figs.5 to 7. With respect to the carbide distributions in each of the four different Si steels,[19] a more heterogeneous distribution with coarser carbides on martensite lath and package boundaries had been found for the higher silicon steels. An example of such a distribution is shown in Fig. 5, where several “large” carbide particles can be observed, whereas the low Si steel presents only a few dark areas, formed by a larger number of small particles. Another important observation is that the large particles in the high Si steel show the same size (between 50 to 150 nm) as the particles observed on the fracture surfaces (Figs. 4a and 4b).

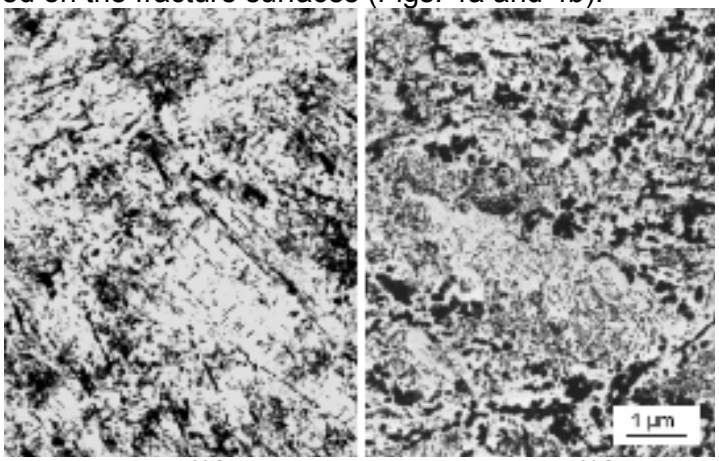


**a)** 0.05%Si **b)** 2.0%Si

**Figure 5.** Carbide distributions after 2x2h tempering for 0.05%Si and 2% Si steels; extraction replicas observed by TEM.

Identification of many carbide particles was carried out, and it was detected that only three types of carbides exist after double tempering for 2+2h at 625ºC (examples shown in Fig. 6): $M_2C$ needles inside the martensite laths of the high silicon steels, but elongated cementite ($M_3C$) carbides in the same regions of the low Si steels; and for both steels the faceted or ellipsoid particles correspond to $M_7C_3$ Cr-rich carbides.

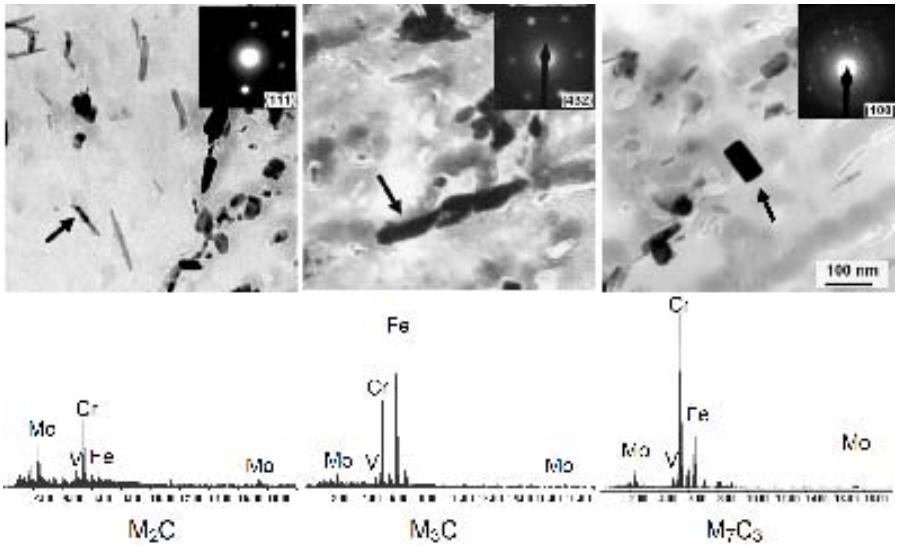


**Figure 6.** Identification of carbides: $M_2C$ in the 2%Si steel, intralath region. Cementite ($M_3C$) found in intralath regions of 0.05%steel. $M_7C_3$ observed mainly in interlath and interpackage regions of all the steels. The reciprocal lattice plane has been identified at the lower right corner of each diffraction pattern.

### 3.4 Early Temperig Stages

The initial stages of carbide formation during tempering are shown in Fig. 7, for the condition 0min at 625ºC (representing the moment when samples reached the tempering temperature for the first time, as mentioned in item 3). It can be seen that elongated cementite particles are present in all regions of the low Si steel microstructures (Fig. 7a), whereas cementite formation is inhibited in the high Si steels. On the other hand, alloy carbides anticipate their formation in high Si steels, either $M_7C_3$ within interlath regions or intralath $M_2C$ (Fig. 7b).

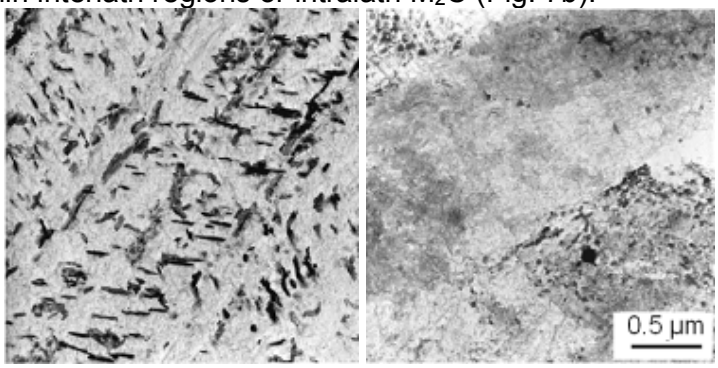


**a)** 0.05%Si **b)** 2.0%Si

**Figure 7.** Carbide distribution in the first tempering stages, for low and high Si steels (same magnificatins), after 0min at 625ºC.

In summary, it can be concluded that cementite formation was suppressed in high Si steels, creating thermodynamic conditions to anticipate the precipitation of alloy carbides. In low Si steels, the first carbide phase formed is cementite, retarding alloy carbide formation. Indeed, from a total of 15 microanalyses of cementite particles in low Si steels, an average stoichiometry of $(Fe_{0.70}Cr_{0.22}Mo_{0.04}V_{0.04})_3C$ was calculated for the particles formed in the early tempering stages. After 2x2h tempering, the remaining cementite particles presented a stoichometry of about

$(Fe_{0.45}Cr_{0.45}Mo_{0.04}V_{0.06})_3C$, indicating an increase of Cr content in solid solution before the cementite particles are dissolved and Cr-rich $M_7C_3$ carbides are formed.

## 4 DISCUSSION

### 4.1 Correlation: Carbide Precipitation and Mechanical Properties

From the mechanical test results (Fig. 1) and fractography analysis (Fig. 2), a correlation between carbide particles and the lower toughness of high Si steels can clearly be deduced. As shown by the carbide distribution analysis, high Si steels tend to present larger carbides on interfaces (interlath and interpackage boundaries), formed more rapidly due to the absence of cementite (more details in ref.[19]). The type of embrittlement is shown to be stronger when fracture surfaces are mainly intergranular (with respect to prior austenite grains), as observed mainly in the higher P steels. Steels with high Si and lower P show a significant increase in toughness (Fig. 1), which is directly related to the modifications found on the fracture surfaces, with the reduction of austenite intergranular areas.

The effect of a high Si content on toughness is thus related to the formation of coarse carbide particles, through a mechanism based on the effect of silicon on cementite formation. As has been long known in the literature,[5-7] cementite formation in high silicon steels is thermodynamically unfavourable[25] and can thus be suppressed. In fact, in a previous paper,[19] the quantity of cementite formed after 0h at 625ºC has been determined for all the four Si levels investigated in the present work, reaching a volume fraction of about 6% for the lower silicon steels, only 3% for the 1%Si and less than 0.2% for the 2%Si steel. Therefore, as cementite is not formed, all the alloy elements that tend to go into solid solution in this phase (especially Cr, with up to 37 at%, as shown before) will still be in solid solution in martensite, in a metastable situation. This thermodynamically condition of alloy elements (and carbon) tends to accelerate the precipitation of alloy carbides, as shown above for the early tempering stages of the higher Si steels (Fig. 7). As diffusion at lower temperatures is crucial for alloy carbide formation, it is then expected that this anticipated precipitation occurs along high diffusion paths, such as prior austenite grain as well as interpackage and interlath boundaries (all grain boundaries with respect to crystallography), thus explaining the concentration of Cr carbides in such regions. Finally, as tempering proceeds, the prematurely formed $M_7C_3$ will grow and become the coarser carbides within the intergranular regions, being identical to the particles found on the fracture surfaces (Fig. 4).

### 4.2 Comparison to TME Models of Low Alloy Steels

The effects of carbide distribution on toughness have been studied extensively in quenched and tempered low alloy steels.[26-28] For lower tempering temperatures, tempered martensite embrittlement (TME) was shown to be caused by cementite formation along the martensite interlath boundaries, frequently but not always[29] due to the decomposition of retained austenite. For alloy steels and higher tempering temperatures, the preferential formation of alloy carbides along the same interlath (and interpackage) boundaries, as observed in the present case, may present a similar microstructure from a toughness perspective, creating preferential locations for fracture initiation or propagation. Therefore, the present mechanism may be considered similar to the mechanism of tempered martensite embrittlement, but the main

role here is played by the distribution of alloy carbides. And as lower silicon contents improve this distribution, the increased toughness of these grades can thus be understood.

Some other factors collaborate with our mechanism of anticipated carbide formation, proposed to explain the lower toughness of higher Si steels. First, the fact that even with lower solid solution hardening (considered to be 4HRC higher in the 2%Si steel), the tempering response of the low Si grades shows the same hardness, meaning that the secondary carbides are in fact finer and better distributed. Second, the higher tempering resistance of low silicon steels, reported in the literature,[10,11] can also be explained by this anticipated carbide precipitation in high silicon steels. In other words, the existence of cementite (still prone to dissolve and re-precipitate carbon in the form of alloy carbides) may be considered as a "reservoir of alloy elements", leading to subsequent hardening after longer tempering times.

### 4.3 The Synergy with Phosphorous

A final explanation from this model allows to understand the effect of phosphorous. When trying to compare our present results to the events of TME in low alloy steels, it should be remembered that, in the case of TME, intergranular fracture on prior austenite grain boundaries was observed in commercial steels but not in high purity steels.[30] Although this intergranular fracture is common for the phenomenon of high temperature temper embrittlement (above 500ºC), due to the segregation of impurity atoms on austenite grain boundaries, it should not be expected to make a difference in the vicinity of 350ºC tempering, due to the low mobility of the substitutional alloying atoms at this temperature interval. A most plausible explanation of the presence of intergranular fracture along prior austenite grain boundaries after low temperature TME is thus the combination of the effects of cementite formation at about 350ºC and the presence of impurity elements that segregated to the grain boundaries during the austenizing treatment.[31,32]

A very similar situation is thus proposed for the present high alloy steels in relation to the P effect. As shown by Ule et al.,[21], phosphorous tends to segregate on grain boundaries and lath regions at temperatures around 500ºC. Therefore, if these regions are subsequently embrittled by coarse $M_7C_3$ particles, intergranular fracture will be enhanced. With lower P levels, although the embrittlement effect of Si is still present, the intergranular areas are reduced. Considering these arguments, the effect of Si (causing coarse $M_7C_3$ on interfaces) and P (causing interface segregation) together can thus explain the synergic effect of Si+P in lowering the toughness. On the other hand, when the interface regions are not embrittled by coarse $M_7C_3$, the P content is less important, thus explaining the weak effect of reducing the P content in low Si steels. Indeed, referring again to the TME mechanism in low alloy steels, the main cause for lower toughness is the preferential origin of cementite formation, but true intergranular fracture is only observed when P (or other embrittling elements) are present on the austenite grain boundaries.[31]

### 4.4 Microstructural Models

In conclusion, the present discussion can be schematically explained by Fig. 8 and Fig. 9, showing the different sequences of precipitation and the final effect on mechanical properties discussed before. Regarding the precipitation sequence, Fig. 8 shows the most important fact related to Si: the earlier cementite formation in

low Si steels (Fig 8a) and the anticipation of $M_7C_3$ carbide formation in high Si steels, causing the coarser distribution (and lower toughness) at higher temperatures [1]. This effect in conjunction to P segregation at higher temperatures is them shown in Fig. 9, representing the synergy of Si and P in the embrittlement mechanism of high Si steels.

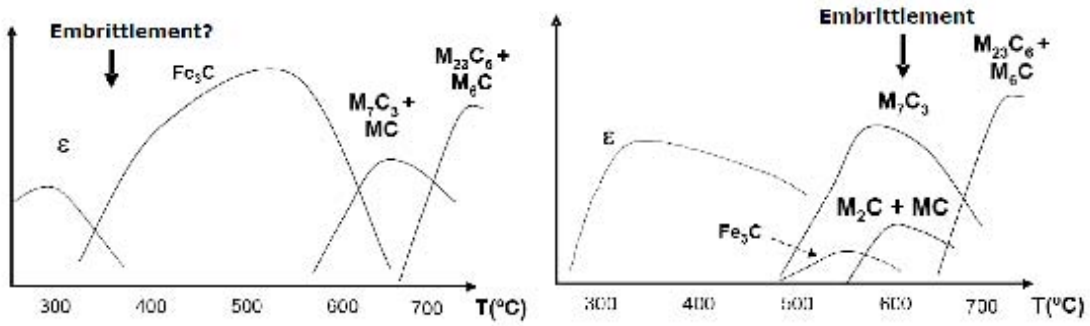


**a)** Low Si **b)** High Si

**Figure 8.** Sequence of precipitation in low and high Si H11. See text for explanation.

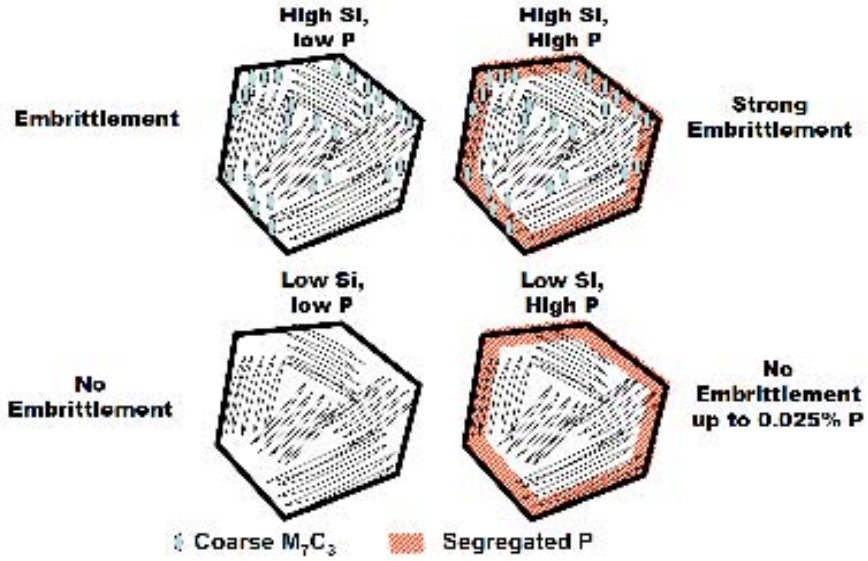


**Figure 9.** Proposed model for the influence of microstructure on the toughness of H11 tool steel, including the effects of Si and P. See text for explanation.

[1] At lower tempering temperatures of low Si steels, the onset of cementite formation would probably cause an embrittlement similar to TME of low alloy steels (as shown by the arrow in Fig 8a), which is not relevant as these grades are tempered be 550ºC [1].

## 5 CONCLUSIONS

- Toughness strongly increases with the reduction of silicon content in H11 tool steel. The increase was shown to be correlated to a better distribution of finer $M_7C_3$ carbides.
- In combination with phosphorous segregation to austenite grain boundaries, the coarser $M_7C_3$ carbides of high silicon steels lead to a stronger embrittlement effect, explaining the importance of both elements for the toughness of traditional high silicon H11 steels.
- Coarser and heterogeneously distributed $M_7C_3$ particles in high silicon H11 steels are related to the early formation of alloy carbides. The event is directly related to the traditional effect of silicon in retarding (or inhibiting) the formation of cementite.
- In the low silicon steels, cementite forms freely within the martensite microstructure, either in inter- or intralath regions.
- As alloy elements, especially Cr, are present in solid solution in cementite, alloy carbide formation in low silicon steels tends to occur after longer times or at higher temperatures. This thus explains the improved tempering resistance of these grades.
- More importantly, the more uniform distribution of previous cementite particles also explains why the subsequent precipitation of alloy carbides is not strongly dependant on high diffusion paths, leading to a finer and more homogeneous distribution of alloy carbide particles.

## REFERENCES

1 G. Roberts, G. Krauss and R. Kennedy: Tool Steels, 5th ed., ASM International, Materials Park, OH, 1998, pp. 220-221.
2 S. Tour: Trans. AIME, 1935, vol. 116, pp. 242-358.
3 J. C. Hamaker Jr: Met. Prog., Dec. 1956, pp. 93-103.
4 B. R. Banerjee: J. Iron Steel Inst., London, 1965, vol. 203, pp. 166-174.
5 A. G. Alten and P. Payson: Trans. Am. Soc. Met.. 1953, vol. 45, p. 498-532.
6 S. Owen: Trans. Am. Soc. Met., 1954, vol. 45, p. 812-829.
7 C. J. Altstetter, M. Cohen and L. Averbach: Trans. Am. Soc. Met., 1962, vol. 55, p. 287-300.
8 W. M. Garrison Jr.: Mater. Sci. Technol., 1987, vol. 3, pp. 256-259.
9 M. Umino, T. Sera, K. Kondo, Y. Okada and H. Tsubakino: Tetsu-to-Hagane (Journal of the Iron and Steel Institute of Japan), 2003, vol. 89, pp. 673-679. (in Japanese).
10 D. Delagnes, P. Lamesle, M.H. Mathon, N. Mebarki, C. Levaillant: Materials Science and Engineering A, 2005, vol. 394, pp. 435-444.
11 R. A. Mesquita, L. C. França and C. A. Barbosa: Proceedings of 57th Congress of Brazilian Materials and Metallurgy Association (ABM), Associação Brasileira de Metalurgia e Materiais, São Paulo, Brazil, 2002. p. 444-453 (in Portuguese).
12 J. Bourrat : US Patent 5,622,674,1994.
13 O. Sandberg, B. Klarenfjord and H. Lindow: Proceedings of 5th International Conference on Tooling – Tool Steels in the Next Century, Leoben, Austria, 1999, pp. 601-610.
14 B. Klarenfjord, O. Sandberg: US Patent 6,365,096, 2002.
15 K.-D Fucks. Proceedings of 6th International Conference on Tooling – The use of tool steels: experience and research, Karlstad, Sweeden, Karlstad University, 2002. pp. 15-22.
16 S. Herbert and F. Kay. US Patent 6,773,662B2, 2004.
17 P. Muhr and I. Siller: Proceedings of 7th International Conference on Tooling – Tooling materials and their application from research to market, Turin, Italy, Politecnico di Torino, vol. 1, 2006, pp. 183-195.

18 R. A. Mesquita and C. A. Barbosa: Tecnologia em Metalurgia e Materiais, São Paulo, 2007, vol. 3, n.3, pp. 63-68. (in Portuguese).
19 R. A. Mesquita, C. A. Barbosa and H.-J. Kestenbach. Accepted to publication in Metallurgical and Materials Transactions A, 2010.
20 R. A. Mesquita, C. A. Barbosa and H.-J. Kestenbach. Submitted to publication in Metallurgical and Materials Transactions A, 2010.
21 B. Ule, F. Vodopivec, M. Pristavec, F. Gresovnik: Mater. Sci. Technol., 1990, vol. 6, p. 1181-1185.
22 R. A. Mesquita and C. A. Barbosa: Metalurgia e Materiais, 2003, vol. 59, p. 17-22 (in Portuguese).
23 R. A. Mesquita, L. C. França and C. A. Barbosa:Tecnologia em Metalurgia e Materiais, 2005, vol. 2, p.70-75 (in Portuguese).
24 C. Ernst. Proceedings of 4th International Conference on Tooling, Bochum, Germany: Ruhr-Universität Bochum, 1996, p. 173-182.
25 H. K. D. H. Bhadeshia: Bainite in Steels: Transformations, Microstructures and Properties, 2nd ed. London: IOM Communications Ltd , 2001. pp. 73-87.
26 M. Sarikaya, B. G. Steinberg and G. Thomas: Metall. Trans A, 1982, vol. 13A, pp. 2227-2237.
27 M. Sarikaya, A. K. Jhingan and G. Thomas: Metall. Trans A, 1983, vol. 14A, pp. 1121-1133.
28 C. L. Briant: Mater. Sci. Technol., 1989, vol. 5, pp.138-147.
29 H.K.D.H.Bhadeshia and D.V. Edmonds: Met. Sci., 1979, vol.13, pp.325-334.
30 C. L. Briant and S. K. Banerji: Metall. Trans. A, 1979, vol. 10A, pp. 1151-1155.
31 J. P. Materkowski and G. Krauss, Metall. Trans. A, 1979, vol. 10A, pp. 1643-1651.
32 C. L. Briant and S. K. Banerji: Int. Met. Rev., v. 23 n. 4, p. 164-199, 1978.